Spacecraft Nutational Instability Prediction by Energy-Dissipation Measurements

S.C. Garg* and N. Furumoto†
Ford Aerospace and Communications Corporation, Palo Alto, California
and
J.P. Vanyo‡
University of California, Santa Barbara, California

Nutational divergence of a spinning spacecraft was studied experimentally and later compard with flight data. Laboratory measurements of liquid energy dissipation in model tanks, with and without propellant management devices, were performed during forced precession of the tanks. Results were used to predict divergence time constants via the energy sink approach and were compared to time constants obtained from flight data. Agreement within 21% was obtained, considered very good since the energy sink approach was used for an exceptionally high liquid-fraction spacecaft. By contrast, analytical estimates were in error by one to three orders of magnitude. Time constants were also compared to drop tests with excellent agreement. Data encompass three designs of propellant management devices and several parameter variations for each design.

Introduction

A MAJOR source of destabilizing energy dissipation in spinning spacecraft is liquid fuel. The amount of liquid fuel, expressed as the ratio of liquid mass to total mass, has become larger with the advent of integral liquid apogee propulsion systems. This ratio will increase dramatically with liquid perigee propulsion stages currently being studied. The simplicity of spin stabilization still means that spinning liquid fuel spacecraft will remain a challenging problem in attitude dynamics and control. The challenges may in fact become greater.

The present work was motivated by the INSAT-1 spacecraft, which carries a liquid apogee propulsion system and is 55% liquid by mass in transfer orbit. A parallel approach prompted by INSAT-1 has been reported previously.[1] The drop tests conducted under that program yielded almost unbelievably short (about 30 s) time constants. The work reported here was done in order to verify at least roughly the energy dissipation concomitant to such short time constants. The specific geometry, viz. two on-axis spherical tanks, lent itself rather well to experimental methods previously developed by Vanyo and Likins.[2,3] Further, the results could be cross-checked against drop test data and eventually against flight data obtained from INSAT-1.

Two numerical estimates of energy dissipation were made by consultants for the INSAT-1 spacecraft. The two, one assuming dissipation only in a spherical laminar boundary layer, and the other based on a numerical approximate solution of the Navier-Stokes equations, differed by two orders of magnitude. Even the larger dissipation estimate was low by nearly a factor of 20 when compared to scale model and flight results. However, it neglected the effect of the PMD (propellant management device) on energy dissipation.

This paper consists of descriptions of scaling; measurement methods; energy-dissipation results; time constant predictions, including comparison of predicted time constants with drop test data and with flight data; and a selection from extensive parameter sensitivity studies. Previous results[4] erroneously placed the flight test data at 45 rpm rather than the actual 40 rpm. Correcting this error leads to better agreement (within 21%) between the forced precession predictions and flight test data.

Received July 12, 1985; revision received Dec. 24, 1985.

*Principal Engineer; presently at COMSAT, Washington, DC. Member AIAA.
†Principal Engineer; presently at Systems Control Technology, Inc., Palo Alto, CA. Member AIAA.
‡Professor, Department of Mechanical Engineering.

Scale Model Principles

Before describing the apparatus, it is important to understand the dimensional analysis principles which enable spacecraft results to be obtained by testing so economically on a small scale in the laboratory.

Consider fluid in a spherical tank subjected to inertial motion corresponding to an axisymmetric rigid body with spin moment of inertia I_s, transverse moment of inertia I_t, initial spin speed ω about the axis of symmetry, and nutation angle θ. Let ρ, μ be the fluid density and viscosity, R the tank radius, g the inertial or gravitational acceleration, and s the liquid surface tension. The tank is assumed to have baffles made of sheet material with flexural rigidity B, and the geometry is completely defined by a dimensionless shape function Γ. The fluid velocity distribution in the tank depends on all the above parameters. Since the energy-dissipation rate $\dot{E}$ is a suitable scalar function of the liquid velocity distribution, we can write

$$\dot{E}=\dot{E}(t,\omega,R,\rho,\mu,g,B,s,\Gamma,\theta) \tag{1}$$

Three fundamental dimensions are involved: mass, length and time. The variables can therefore be reduced by three using the "pi theorem." This yields a dimensionless normalized energy-dissipation function f:

$$f=\dot{E}/\rho\omega^3R^5 \tag{2a}$$

$$f=f(\omega t,\ \omega R^2/\mu,\ \omega^2R/g,\ B/\rho R^6\omega^2,\ s/\rho gR^2,\ \Gamma,\ \theta) \tag{2b}$$

The quantities in the parentheses are dimensionless time, Reynolds number Re, Froude number F, baffle stiffness parameter K', Bond number b, dimensionless shape function, and nutation angle, respectively. Note in Eq. (2a) that the energy-dissipation rate $\dot{E}$ is a function of θ only through the normalized function f.

The three-dimensional shape function Γ does not appear explicitly in the following analysis. It represents the geometric similarity between the vehicle tank and the model tank which is scaled in all respects with one important exception. The baffle sheet thickness h is chosen to scale the baffle stiffness rather than Γ. This is justified below. Assuming further a nominal steady state condition and negligible surface tension effects gives

$$f=f(Re,F,K',\theta) \tag{3}$$

where the variables f, Re, F and K' are defined following Eqs. (2a) and (2b).

The baffle stiffness parameter K' is important if a propellant management device or baffle exsits for any reason. Flexural rigidity B depends on the baffle geometry and material properties. For thin planar baffles fixed at the tank wall, B is related to baffle deflection when a unit force is applied at the free end, and is proportional to $E_y wh^3$, where E_y is Young's modulus of elasticity and w and h are the baffle width and thickness, respectively. After substituting into the definition in (2b)

$$K' \sim E_y wh^3/(\rho R^6\omega^2) \tag{4}$$

When scaling K', all test variables, except E_y and h, are fixed by other scaling parameters. Young's modulus is fixed by selection of sheet material with sufficient yield limits, and the baffle thickness h is then selected to match K'. In this way, h will not necessarily match the thickness component of the shape function Γ. Since the thickness of the baffle is much smaller than the tank radius, and since surface tension effects are of little consequence at the spin speeds that are of interest, the use of thickness to control stiffness at the expense of the shape function appears justified.

A suitable model thus contains a scaled tank, scaled baffles (including stiffness), and a fluid of appropriate viscosity and density so that the proper Reynolds number is obtained at a reasonable spin speed. This tank is then subjected to precession speeds of $\dot{\phi}=\sigma\omega$ and spin speeds of $\dot{\psi}=(1-\sigma)\omega\cos\theta$ where σ is the inertia ratio I_s/I_t of the candidate spacecraft and θ a given nutation angle.

Our assumption is that if Re, F, K', and θ of Eq. (3) are the same for both the tests and the spacecraft, the dimensionless energy-dissipation functions (f) are the same. The test values of $\dot{E}$ are then scaled using $(f\rho\omega^3R^5)$ for the tests and for the spacecraft to give predicted spacecraft $\dot{E}$. This predicted spacecraft $\dot{E}$ is then used to compute a predicted spacecraft nutation divergence time constant.

Spacecraft Nutation Divergence

The nutation divergence time constant (τ) of a spinning vehicle is related to energy dissipation within the vehicle using the energy sink model. This model is based on the motion of a torque-free, inertially axisymmetric rigid body. It relates changes in rotational kinetic energy of the body (E) to changes in the nutation angle (θ) while angular momentum is kept constant. Although $\dot{E}$ and $\dot{\theta}$ are zero for a rigid body, an assumption is made that if $\dot{E}$ and $\dot{\theta}$ are small in the real object, the model will be adequately valid. The $E=E(\theta)$ relationship is differentiated with respect to time to give $\dot{\theta}$ as a function of $\dot{E}$. After assuming θ small and defining τ as the ratio $(\dot{\theta}/\theta)$, the energy-sink method yields

$$\tau=I_s(1-\sigma)\omega^2/(\dot{E}/\theta^2) \tag{5}$$

If $\dot{E}/\theta^2$ is essentially constant over portions of the range of θ, then τ is also constant, and nutation divergence is exponential ($e^{t/\tau}$) over those values of θ. An assumption of constant τ is often made for convenience. Note that τ is positive for slender configurations ($\sigma<1$) so that $\theta(t)$ diverges. Convergence results for $\sigma>1$. As used here, $\dot{E}$ is positive for a system losing energy.

The energy sink model assumptions are clearly violated when applied to large liquid mass fraction vehicles where $\dot{E}$ and $\dot{\theta}$ can be large. Moreover, the axisymmetric assumption is compromised because of sloshing liquids. Problems can occur with fluid resonances and baffle resonances, which can cause sharp changes in $\dot{E}$ over a range of initial spin rates ω. This makes predictions risky as seen on some past spacecraft.[5] A further complication is the fluid-structure interactions which occur in the case of multiple tanks. Thus, judgment and discretion should be exercised in using energy-sink and dissipation measurements only. One of the purposes of this work was to compare such results with other estimates and with flight data.

In relating tank tests to spacecraft divergence, a functional relationship for spacecraft $\dot{E}$, as suggested by Eqs. (1), (2), and (3), must be assumed. Following Eq. (2a) we have

$$\dot{E}=f\rho\omega^3R^5 \tag{6}$$

If $f\sim\theta^n$ where $n\neq 2$, τ will depend on θ, and divergence will be nonexponential. In some results reported below, such was found to be the case. Other tests[3] have indicated laboratory $\dot{E}$ proportional to $\sin^2\theta$, approaching θ^2 for small θ. In this analysis, $\dot{E}$ is a function of θ through the dependence of f upon θ. An earlier paper[4] had used an explicit $\dot{E}(\theta)$.

Equation (6) is consistent with an earlier mathematical model developed by Vanyo[6] for dimensionless energy dissipation. A transformation from a 7-D experimental space to a 2-D analytical space applied to many thousand data points yielded the following equation, with (p) an alternate dimensionless energy dissipation parameter

$$\dot{E}\sim p\rho\omega_t^2\omega_s R^5/(1+\zeta^2) \tag{7}$$

Here, ω_s and ω_t are the secular and transient components of the vehicle inertial angular velocity, and ζ is an Ekman number ($\sim Re^{-1}$) based on a boundary layer thickness $\delta\sim(\nu/\omega_s)^{1/2}$ as characteristic length and $R\dot{\phi}$ as characteristic velocity. It can be interpreted as a ratio of viscous to transient inertial forces. After use of the energy sink approximations, and provided θ is small and $(\nu/\omega)^{1/2}\ll R\sigma$, $(1+\zeta^2)$ reduces to one, and Eq. (7), with $f=p\theta^2(1-\sigma)^2$, reduces to Eq. (6).

The condition on $(\nu/\omega)^{1/2}$ says merely that the thickness of the viscous boundary layer (e.g., Ekman layer or depth of penetration in Stokes' solution for an oscillating flat plate) be small relative to $R\sigma$. The ratio $(\nu/\omega)^{1/2}/R\sigma$ is very small for INSAT-1 and all typical communication satellites in a spinning mode. The smallness of this ratio helps to explain the inadequacy of numerical solutions based on a laminar dissipation mechanism. Turbulence dominates $\dot{E}$ for all practical vehicle tank sizes, fluids and angular velocities.

After substituting $\dot{E}$ from Eq. (6) into Eq. (5), one obtains

$$\tau=I_s(1-\sigma)\theta^2/(f\rho\omega R^5) \tag{8}$$

with all variables, including f, appropriate for the spacecraft. Laboratory forced precession $\dot{E}$ results are now introduced by equating spacecraft f values to laboratory f values previously obtained from Eq. (2a). This is valid since laboratory parameters are chosen to match the experimental nondimensional parameters of Eq. (3) to those of the spacecraft. In particular, for $\dot{E}/\theta^2$ not constant, the nutation angle of the laboratory tests must correspond to the average θ of the spacecraft. For systems with more than one tank, the energy dissipation function $\dot{E}$ represents the sum of all the energy dissipation sources with each tank tested separately at the same θ. Finally, an equation predicting spacecraft τ is obtained by combining Eq. (8) with Eq. (2a) and carefully

distinguishing between laboratory and spacecraft quantities

$$\tau = I_s(1-\sigma)\omega^2\theta^2/(\rho_r\omega_r^3 R_r^5 \dot{E}) \tag{9}$$

In this equation, $\dot{E}$ is the total energy dissipation measured in the laboratory at angle θ, and the subscript (r) refers to ratios of spacecraft flight parameters to equivalent laboratory test parameters. These ratios scale the laboratory $\dot{E}$ to predicted spacecraft $\dot{E}$. All the other quantities are spacecraft parameters including the predicted spacecraft nutation divergence time constant τ. Compare Eq. (9) with Eq. (5).

Laboratory $\dot{E}$ Measurement

The test apparatus at the University of California, Santa Barbara, Rotating Fluids Laboratory is shown schematically in Fig. 1. It consists of a hollow spin body assembly (b), an inner gimbal assembly (e), an outer gimbal (g), a vacuum housing and support structure (n), and associated instrumentation. The angles ϕ, θ, ψ establish a sequence of rotations from the support frame n (considered a Newtonian or inertial frame) through the outer and inner gimbal frames g and e to the spin body b.

The mechanism is designed to maintain the angle θ at a constant value, while permanent magnet dc motors maintain (in the steady state) the virtual constancy of spin rate $\dot{\psi}$ and precession rate $\dot{\phi}$. The motors are calibrated to correlate measured input current with output torque, which then provides a measure of power flow into the system.

Two modes of operation are possible. In the first mode, the apparatus is operated with b empty over the desired range of kinematical variables $\dot{\phi}$, $\dot{\psi}$, and θ; then the cavity is filled, and the exact same series of tests is repeated. In both cases, the $\dot{\phi}$ and $\dot{\psi}$ motor currents are recorded. These are transformed into motor turques through the calibrated torque/current curves. The empty steady state results are subtracted from the liquid-filled steady-state results through a careful procedure designed to compensate for changes in bearing friction due to fluid mass, and the results are the torques required to maintain the liquid in a steady-state motion. The torques are then transformed into energy dissipated in the liquid by the equation:

$$\dot{E} = M_s\dot{\psi} + M_p\dot{\phi} \tag{10}$$

Here, $\dot{E}$ is the energy dissipated because of the liquid motion and M_s and M_p are the liquid filled minus empty spin $(\dot{\psi})$ and precession $(\dot{\phi})$ net motor torques, respectively.

Because the $\dot{\phi}$ motor does not contribute to $\dot{E}$ in steady-state conditions,[2,3] a simpler procedure uses only the equation

$$\dot{E} = M_s\dot{\psi} \tag{11}$$

In this mode of operation, first $\dot{\phi}$ is zero and a steady state $\dot{E}$ is recorded after spin-up to a fixed value of $\dot{\psi}$. Under these conditions, the fluid experiences nearly rigid body motion so all measured M_s is due to parasitic losses. For a partially filled tank, the Froude number must be adequately large ($\gtrsim 40$) to minimize effects of Earth gravity. After recording M_s for $\dot{\phi}=0$, $\dot{\phi}$ is set to a desired value and M_s is again recorded for the new steady state condition. The difference between $\dot{\phi}=0$ and $\dot{\phi}$ as desired provides net M_s for use in Eq. (11). When $\dot{\phi}$ and $\dot{\psi}$ both are so large that gyroscopic moments seriously affect parasitic bearing losses ($\dot{\psi}\sim 2000$ and $\dot{\phi}\sim 1000$ rpm), the first mode of operation is used.

The success of either approach depends crucially on accurate calibration of spin and precession motor characteristics and careful control of parasitic frictional losses. The considerable experience (many thousand data points) gathered by Vanyo et al[7] was very useful here. Allowance for bearing heat-up was made by taking several readings of one condition and discarding the ones near the beginning of a run. Finally, for INSAT-1, dissipation rates measured were about an order of magnitude greater than parasitic friction, making dissipation measurements easier.

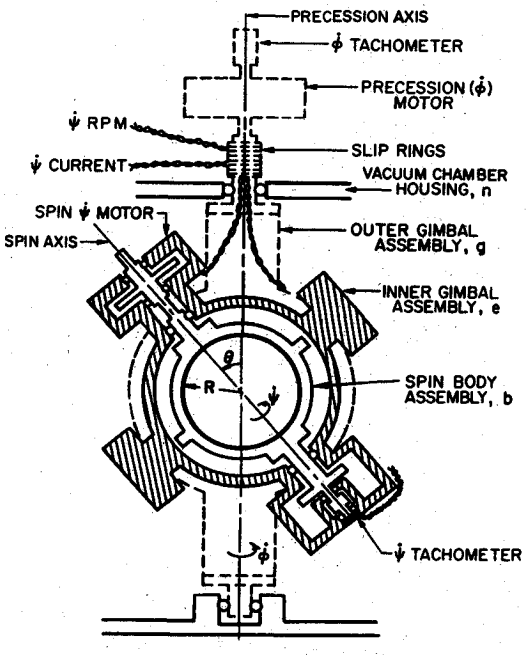

Fig. 1 Experimental apparatus.

Table 1 Spacecraft parameters

Parameter	Spacecraft A Pre-PAM[a] burn	Spacecraft B Pre-PAM burn	Spacecraft C Pre-PAM burn
$I_s \sim$ kg-m^2	699.9	788.7	699.9
$I_t >$ kg-m^2	3990.0	3849.7	3990.0
$\sigma = I_s/I_t$	0.175	0.205	0.175
$\omega \sim$ rpm	45	45	45
$R \sim$ m	0.419	0.435	0.419
$M_{\text{fluid}} \sim$ kg	620	666	620
$M_{\text{Total}} \sim$ kg	3291	3431	3291
Re (Oxidizer)	2.87×10^6	3.075×10^6	2.87×10^6
Re (Fuel)	0.76×10^6	0.811×10^6	0.76×10^6
K (Oxidizer)	14.9×10^{10}	13.7×10^{10}	Rigid PMD
K (Fuel)	1.71×10^{10}	1.56×10^{10}	
Fluid characteristics	$\rho_{OX}=1.45\times10^3$ kg/m^3, $\nu_{OX}=0.29\times10^{-6}$ m^2/s		$\rho_F=0.877\times10^3$ kg/m^3, $\nu_F=1.10\times10^{-6}$ m^2/s

[a]Payload assist module, a perigee stage.

Application to Spacecraft

The present method was first applied to the INSAT-1 weather and communications satellite for India. This spacecraft contains two on-axis spherical tanks with flexible propellant management device (PMD) vanes. One tank contains monomethyl hydrazine (MMH) as fuel, and the other contains nitrogen tetroxide (N_2O_4) as oxidizer. At a given spin rate, the two fluids have different Reynolds numbers and different PMD stiffness parameters. Consequently, the two tank models must be tested separately and different liquids must be used in general to simulate dimensional similarity. Tests to date have made use of isopentane, chloroform, alcohol, acetone, water, and various silicone liquids. The first two were discontinued for safety reasons. Total energy dissipation is obtained by summing separate measurements from two tanks. Finally, this data must be used to estimate the nutation divergence time constant τ for an unstable spinner, using Eq. (9).

Results on the effect of fuel slosh on nutational stability are presented for INSAT-1 (termed spacecraft A hereafter) and

two other spacecraft designs labelled spacecraft B and C. Their parameter values are shown in Table 1. The parameter K of Table 1, and the following figures, is computed as

$$K = K' Re^2 \tag{12}$$

The fuel and oxidizer tanks are aligned along the nominal spin axis for all spacecraft designs considered here. The PMD for spacecraft A is made up of thin titanium sheets forming a vane-like device with its central axis tilted 30 deg from the nominal spin axis. For spacecraft B, the PMD is of similar design and is aligned along the nominal spin axis. The latter case should result in lower energy dissipation rates, essentially because the bulk of the PMD will be in the cylindrical ullage of the fluids until the nutation angle becomes relatively large (10 deg or more). In addition to the two PMD designs made of vane-like sheets, a rigid, conically shaped PMD design for spacecraft C was tested. This PMD occupied about the lower one-third of the spherical test tank.

To assure that zero gravity conditions are approached, the normalized energy dissipation rate was measured as the Froude number was increased. Ideally, zero gravity conditions are reached as the Froude number approaches infinity. Figure 2 shows that for the simulated spacecraft A, Froude numbers greater than 40 are sufficiently high to assure that nearly zero-g conditions have been reached. Note that F is Froude number and FF is fraction fill. Similar runs were made to establish the appropriate Froude numbers for the other simulated spacecraft.

Figure 3 shows the normalized dimensionless energy dissipation function f as a function of Reynolds number for spacecraft A. The Froude numbers are high enough that changes in f would be due to Reynolds number only. The results obtained for fuel and oxidizer $\dot{E}$ are summed and substituted into Eq. (9), along with other data, and the spacecraft nutation divergence time constant is determined to be 55 s at a spin rate of 40 rpm and nutation angle of 5 deg. The same method was applied to obtain time constants for all cases. This approach neglects any changes in dissipation due to interaction between the two tanks.

Spacecraft time constants derived by this method (forced precession experimental measurements of f) are shown in Fig. 4 for spacecraft A and also for spacecraft B, with PMD aligned along the spin axis. As expected, spacecraft B diverges less rapidly. There are two comparison point-sets of interest, also shown in Fig. 4. For spacecraft A, flight data were obtained from perigee stage telemetry. The time constant at 40 rpm deduced from filtered flight data was 69.5 s,[8] compared to the present approach, which gives 55.0 s, about 21% lower than the flight value. The second comparison is made with drop tests described in Ref. 1. In brief, a drop test consists of a properly scaled model of the entire spacecraft which is spun-up and dropped from a height, giving a free-fall time of about 1 s. As Fig. 4 shows, both the forced precession and the drop-test results agree very well with the flight data. This indirect verification is useful when evaluating the results for other vehicles, e.g., spacecraft B, for which no flight data are available. Forced precession $\dot{E}$ results of earlier tests,[3] using the same test apparatus, have recently been found to agree with test data of Zedd and Dodge,[9] who measure fluid forces and moments rather than $\dot{E}$.

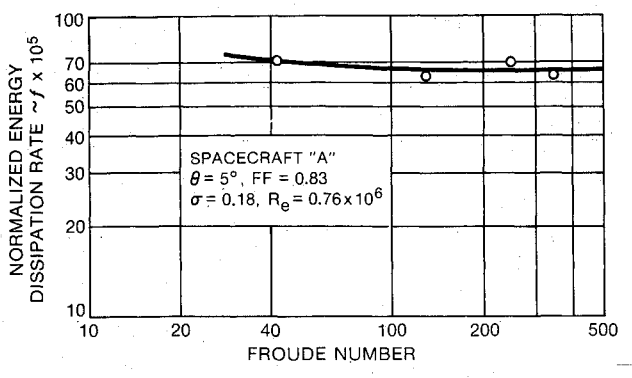

Fig. 2 INSAT energy-dissipation rate variation with Froude number.

Sensitivity Studies

Because of the simplicity of the forced precession tests, a number of different conditions can be run easily and rapidly to determine the sensitivity of the fluid energy-dissipation rate

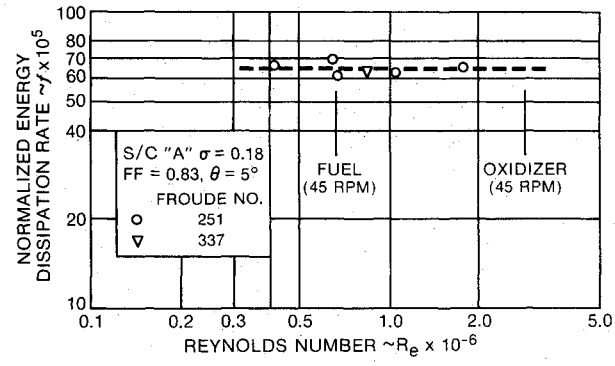

Fig. 3 INSAT energy-dissipation rate variation with Reynolds number.

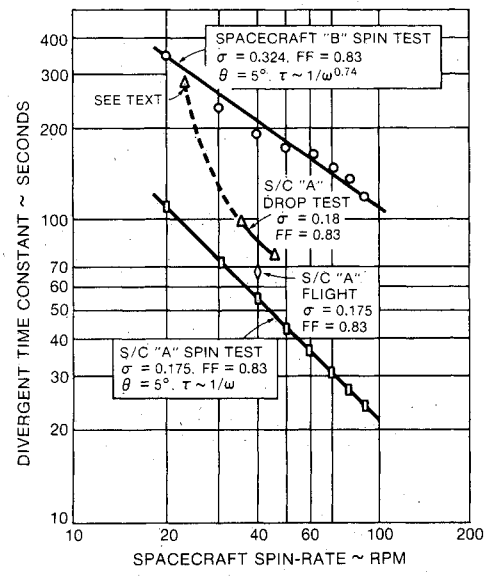

Fig. 4 Effect of spin rate on divergent time constant.

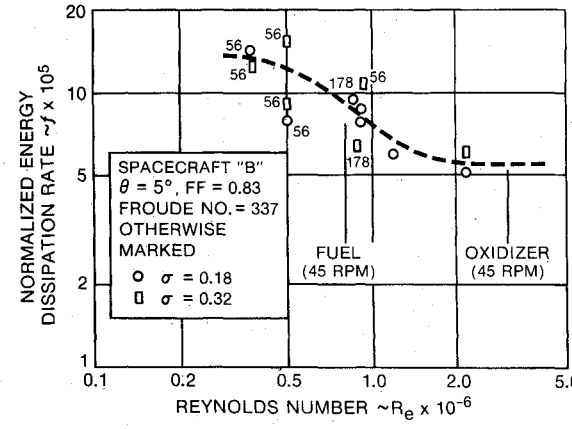

Fig. 5 Spacecraft B energy-dissipation rate variation with Reynolds number.

to various parameters. This is a major advantage and is exploited in the present work.

For spacecraft A, the normalized energy-dissipation rate f of the simulated model tank was found to be independent of the Reynolds number over the range 0.4×10^6 to 2.0×10^6 (Fig. 3). This causes the nutational divergence time constant to be nearly inversely proportional to the spin rate, as seen in Fig. 4. Although the drop tests showed a deviation from this inverse proportionality at lower spin rates, this was probably due more to the difficulty of measuring longer time constants than to Reynolds number effects. The observed insensitivity of the normalized energy-dissipation rate to Reynolds number also minimizes the effect of moderate discrepancies in matching fluid properties. For values of Reynolds number typically in the millions (as for spacecraft A), turbulent flow is fully developed. This insensitivity to Reynolds number is also in accord with the findings of Neer and Salvatore,[10] where at the higher energy-dissipation rates (50% fraction fill) the energy-dissipation rate is virtually independent of Reynolds number, whereas at the lower energy-dissipation rates (lower fraction fills), a definite dependence upon Reynolds number was observed.

For spacecraft B, the function f is plotted vs Reynolds number in Fig. 5. Froude numbers for these points, although different, are high enough to minimize gravity effects. The data show a strong dependence of f on Re for spacecraft B. Hence, rather than an inverse relationship of τ to the spin rate, τ is found to be approximately proportional to the spin rate raised to the negative 0.74 power (see Fig. 4).

The dependence of normalized energy-dissipation rates on nutation angle was studied for spacecraft A. The dissipation

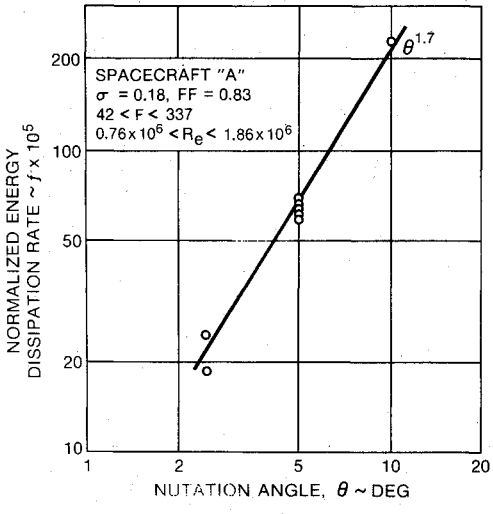

Fig. 6 INSAT energy-dissipation rate variation with nutation angle.

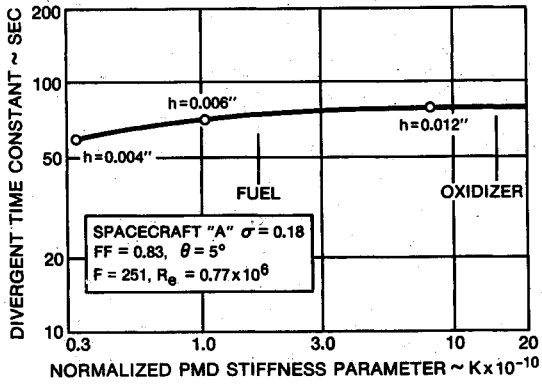

Fig. 7 Effect of PMD stiffness on divergent time constant.

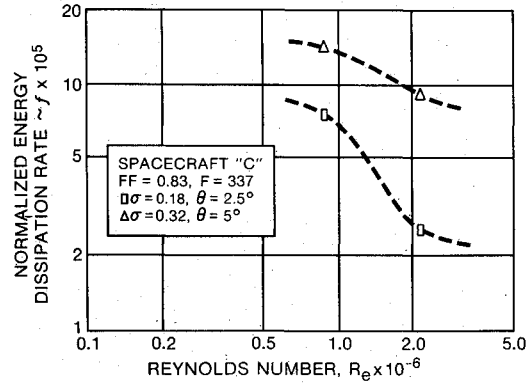

Fig. 8 Spacecraft C energy-dissipation rate variation with Reynolds number.

function f varied as the 1.7 power of the nutation angle as shown in Fig. 6. If it varied directly as the 2.0 power, the divergent time constant would be independent of the nutation angle; see Eq. (8). Since the portion of the PMD immersed in the fluid would vary as the nutation angle varies, devaition of dissipation rates from the second power of the nutation angle is not unexpected. This implies non-exponential divergence. The effect of F and Re on f is negligible in the range shown.

Figure 7 shows the variation of divergent time constant with the normalized stiffness parameter of the vane-like PMD for spacecraft A. For particular Reynolds numbers, only slight increase in the divergent time constant is observed with increasing stiffness parameter. This shows that, although care should be taken to match PMD stiffness parameters of the model to those of the spacecraft, some variations can be tolerated.

Figure 8 plots normalized energy-dissipation rate as a function of Reynolds number for spacecraft C. This figure shows a distinct reduction of normalized energy dissipation at the higher Reynolds number, as also observed in Fig. 5 for spacecraft B. Vanyo et al.[7] found for spherical tanks at Reynolds number below approximately 50 and above about 0.5×10^6, the energy-dissipation rate is independent of Reynolds number. These two limits probably correspond to laminar and fully developed turbulent flows, respectively. Between these limits, they observed that the energy-dissipation rate varied as $Re^{-1/2}$. This suggests that the dependence on Re shown in Figs. 5 and 8 is very similar to that of a tank with no PMDs. This is not surprising, since the PMDs for spacecraft B and C are much smaller than those for spacecraft A. Also, the overall magnitudes of the dissipation rates are considerably smaller than that for spacecraft A, due primarily to the differences in the PMD designs noted earlier. The variation with Reynolds number implies that the divergence time constant is no longer inversely proportional to spin rate. These observations are consistent with laminar fluid flow transitioning to turbulent flow at the higher Reynolds number. One infers that for spacecraft A, fully developed turbulent flow accounts for energy dissipation over the entire range of parameters tested.

Conclusions

Spacecraft nutational stability characteristics have generally been established by costly air-bearing tests with full-scale or nearly full-scale models of the spacecraft tanks. These work well with divergent time constants $\sim10^3$ s. Drop tests, described in detail in Ref. 1, work best for τ an order of magnitude lower, although 10^3 s may be possible. Both drop tests and energy-dissipation tests are much less expensive than the air-bearing tests. Drop tests and the $\dot{E}$ tests of this paper can be combined to provide sufficiently accurate, simple and highly cost effective scaled measurements of nutational instability due to fuel slosh. In addition, the forced precession tests can provide a complete sensitivity study to assure that

stability characteristics can be predicted in the presence of parameter variations due to flight conditions.

For the INSAT-1 spacecraft in the post-perigee burn condition, the forced precession tests rendered credible the extremely short (about 30 s) nutation divergence time constants obtained in the drop tests. The high degree of instability was turned into an advantage in that no attempt at automatic nutation control was made after perigee injection, allowing the spacecraft to diverge to major axis spin prior to despin and sun acquisition. At that time, this mission plan was unique to INSAT-1 and relied on the time constant estimates from drop tests, supported by the forced precession data. As predicted, the spacecraft reached major axis spin within five minutes after perigee injection. Reliance on the analytical estimates alone would have made this spin condition totally unexpected. Mission plans similar to the INSAT-1 plan have since been employed on other spacecraft as well.

Tests conducted to date have been for inertially symmetric configurations. However, off-axis tank configurations can be tested by putting them in an inertially symmetric housing. Tests conducted at high Reynolds numbers have required spin speeds up to 2700 rpm, due to the limited size of the faciltiy. A larger facility is contemplated at the University of California, Santa Barbara which will increase the range of problems addressable by this approach. It is hoped that the forced precession energy dissipation technique will be found useful for other spacecraft.

Acknowledgment

Publication of this paper was supported in part by the Communications Satellite Corporation (COMSAT), Washington, DC.

References

[1]Harrison, J.A., Garg, S.C., and Furumoto, N., "A Free-Fall Technique to Measure Nutation Divergence, and Applications," AIAA Paper 83-372, Aug. 1983.

[2]Vanyo, J.P. and Likins, P.W., "Measurement of Energy Dissipation in a Liquid-Filled, Precessing Spherical Cavity," *Journal of Applied Mechanics,* Vol. 38, Sept. 1971, pp. 674-682.

[3]Vanyo, J.P., "An Energy Assessment for Liquids in a Filled Precessing Spherical Cavity," *Journal of Applied Mechanics,* Vol. 40, Dec. 1973, pp. 851-856.

[4]Garg, S.C., Furumoto, N., and Vanyo, J.P., "Measurement of Energy Dissipation in Forced Precession Compared to Flight Data," AIAA Paper 84-1841, Aug. 1984.

[5]Slabinski, V., "Intelsat-IV In-Orbit Liquid Slosh Tests and Problems in the Theoretical Analysis of the Data," *COMSAT Technical Review,* Vol. 8, Spring 1978, pp. 1-40.

[6]Vanyo, J.P., "Transformation from a 7-Dimensional Experimental Space for Precessing Fluid Energy to a 2-Parameter Analytical Space," *Journal of Applied Mechanics,* Vol. 41, Dec. 1974, pp. 1128-1130.

[7]Vanyo, J.P., Lu, V.C., and Weyant, T.F., "Dimensionless Energy Dissipation for Precessional Flows in the Region of $Re=1$," *Journal of Applied Mechanics,* Vol. 42, Dec. 1975, pp. 881-882.

[8]Garg, S.C., "INSAT-1A Flight Data on Tau," FACC Internal Memo, March 1983.

[9]Zedd, M.F. and Dodge, F.T., "Energy Dissipation of Liquids in Nutating Spherical Tanks Measured by a Forced Motion-Spin Table," *Naval Research Laboratory Report,* NRL 8932, Oct. 1985.

[10]Neer, J.T. and Salvatore, J.O., "Fuel Slosh Energy Dissipation on a Spinning Body," Hughes Aircraft Company Report SCG 20047R, Los Angeles, Feb. 1972.